PHYSICAL REVIEW D

PARTICLES AND FIELDS

THIRD SERIES, VOLUME 42, NUMBER 11 1 DECEMBER 1990

Cosmic-ray muons in the deep ocean

J. Babson,[e] B. Barish,[b] R. Becker-Szendy,[e] H. Bradner,[d] R. Cady,[e,*] J. Clem,[h] S. T. Dye,[e,†] J. Gaidos,[f] P. Gorham,[e,‡] P. K. F. Grieder,[a] M. Jaworski,[i] T. Kitamura,[g,§] W. Kropp,[c] J. G. Learned,[e] S. Matsuno,[e] R. March,[i] K. Mitsui,[g] D. O'Connor,[e] Y. Ohashi,[g] A. Okada,[g] V. Peterson,[e] L. Price,[c] F. Reines,[c] A. Roberts,[e] C. Roos,[h] H. Sobel,[c] V. J. Stenger,[e] M. Webster,[h] and C. Wilson[f]

(DUMAND Collaboration)

[a]*University of Bern, Bern, Switzerland*
[b]*California Institute of Technology, Pasadena, California 91125*
[c]*University of California at Irvine, Irvine, California 92717*
[d]*University of California at San Diego, Ja Jolla, California 92093*
[e]*Hawaii DUMAND Center, University of Hawaii, Honolulu, Hawaii 96822*
[f]*Purdue University, Layfayette, Indiana 47907*
[g]*Institute for Cosmic Ray Research, University of Tokyo, Tokyo, Japan*
[h]*Vanderbilt University, Nashville, Tennessee 37215*
[i]*University of Wisconsin, Madison, Wisconsin 53706*

(Received 2 January 1990)

A string of seven optical detectors deployed from a ship was used to detect the Cherenkov light from muons at ocean depths ranging from 2000 to 4000 m in intervals of ~500 m. The flux and angular distributions of cosmic-ray muons were measured. An effective area for fivefold coincidences of 420 m^2 for downward-going muons was achieved. The results are consistent with those derived from underground observations and theoretical calculations. The measured vertical intensity ranges from $(9.84\pm6.5)\times10^{-8}$ $cm^{-2}s^{-1}sr^{-1}$ at 2090 m of water equivalent (mwe) to $(4.57\pm1.37)\times10^{-9}$ $cm^{-2}s^{-1}sr^{-1}$ at 4157 mwe.

I. INTRODUCTION

Measurements of the cosmic-ray muon energy spectrum and lateral distribution provide information on the spectrum and composition of primary cosmic rays and on the interaction between the primary-cosmic-ray particles and the nuclei in the atmosphere. Spectra for vertical and horizontal muons have been measured by magnetic spectrometers.[1-5] Although these provide a straightforward way to determine muon momenta, they are limited in detection area, angular acceptance, and maximum detectable momentum (<1 TeV/c for vertical muons, ≤ 20 TeV/c for horizontal ones).

To complement magnetic spectrometers, the muon spectrum can be directly measured by means of the depth-intensity relation of muons in underground experiments.[6-8] By measuring the muon flux at different depths, or the zenith angular distribution at a given depth, the muon intensity as a function of the thickness of matter traversed can be obtained. Since a certain minimum energy at sea level is required for a muon to reach a given depth, measurements at varying depths allow one to explore the high-energy end of the sea-level muon spectrum.

Underground experiments are limited in size and by the variability and uncertainty in the rock composition above the detector. These problems can be overcome by measurements underwater, where large detection volumes are possible using the water itself as a detection medium, and where the matter overburden is well known and highly homogeneous. For seawater $\rho=1.027$ $g\,cm^{-2}$, $\langle Z\rangle=7.47$, $\langle A\rangle=14.87$, $\langle Z/A\rangle=0.5525$, $\langle Z^2/A\rangle=3.77$, where ρ is the mean density, Z is the atomic number, and A the atomic weight.[9]

Deep-ocean water is remarkably clear, so it can be used as a Cherenkov radiator to detect relativistic charged particles. The attenuation length of blue light in water can be as great as 40 m.[10-11] Until recently, underwater measurements have been limited in effective area when compared to underground measurements.[12-15] Previous

experiments measure muon intensity by recording the local coincidence rate of several light sensors, assuming that the coincidences were caused only by muons. To date, muon trajectory reconstruction and muon angular distributions have not been carried out in deep-ocean experiments.

Presented here are the results of first stage experiments for the DUMAND (Deep Underwater Muon And Neutrino Detector) project.[16] The ultimate aim of DUMAND is to build a detector in the deep ocean capable of searching for point source of high-energy neutrinos of astrophysical origin. Cosmic-ray muon vertical intensity vs depth, and muon angular distribution vs depth were measured in the ocean off the West coast of the island of Hawaii in November 1987. Measurements were made at depths ranging from 2000 to 4000 m in intervals of 500 m with an instrument called the short prototype string. The short prototype string demonstrates the technical feasibility of using the water Cherenkov technique in the ocean, to detect muons and to reconstruct their trajectories. This is a critical test for the DUMAND project, since neutrinos are to be detected by reconstructing upward-directed muon trajectories.

Considerable data on the deep-ocean environment and light backgrounds were obtained in this experiment.[17] The principal source of background is Cherenkov radiation from the β decay of ^{40}K in seawater, which contributed a noise rate in the phototubes of 20.9 ± 1.6 kHz, at the one-photoelectron level.

II. APPARATUS

The entire short prototype string array employed seven optical modules, two calibration light-source modules, a multipurpose environmental sensor module, two hydrophones, an instrumentation module, and a string bottom controller. Data from the various modules were sent to the string bottom controller by means of individual multimode fiber-optic cables. Upon reaching the string bottom controller, these data were digitized, encoded, multiplexed, and then transmitted serially at 50 Mbaud to the ship through a single-mode fiber optic cable. Onboard ship, the data were received, decoded, selected, and recorded on magnetic tape, using a CAMAC data-acquisition system controlled by a PDP-11/73 computer.

The seven optical modules (shown in Fig. 1) are evenly spaced 5.18 m apart along the length of the string. The calibration modules are located on the string between the second and third optical modules, and between the fifth and sixth optical modules. The length of the string, measured from the top optical module to the bottom optical module, is 30.6 m. Technical details and performance of the individual instruments are discussed elsewhere.[18,19]

When a relativistic muon passes in the vicinity of the string, the resulting Cherenkov wave front can hit several optical modules within a time window of < 100 ns. In the string bottom controller, this light is detected by a 38-cm-diameter hemispherical photomultiplier tube[20] enclosed in an optically clear high-pressure housing. The analog output pulse from the photomultiplier tube is amplified and encoded in the optical module to a pulse such that the leading edge of the pulse represents the arrival time, and the duration of the pulse is proportional to the logarithm of the intensity of the light. Typically, a single photoelectron gives a pulse width of 100 ns. The overall instrumental time resolution is 10 ns full width at half maximum for a 1-photoelectron pulse, and improves to 6-ns full width at half maximum for a 10-photoelectron pulse. Light intensity is determined with a resolution $^{+100}_{-50}\%$ for a range of light levels from 1 photoelectron to a few tens of photoelectrons.

Fast timing and photomultiplier tube stability calibration are provided by the calibration module. The latter consists of a 337-nm pulsed nitrogen laser, operator selectable neutral density filters, and control circuitry enclosed in a glass pressure housing of 43 cm diameter. The output pulse [2 ns full width at half maximum

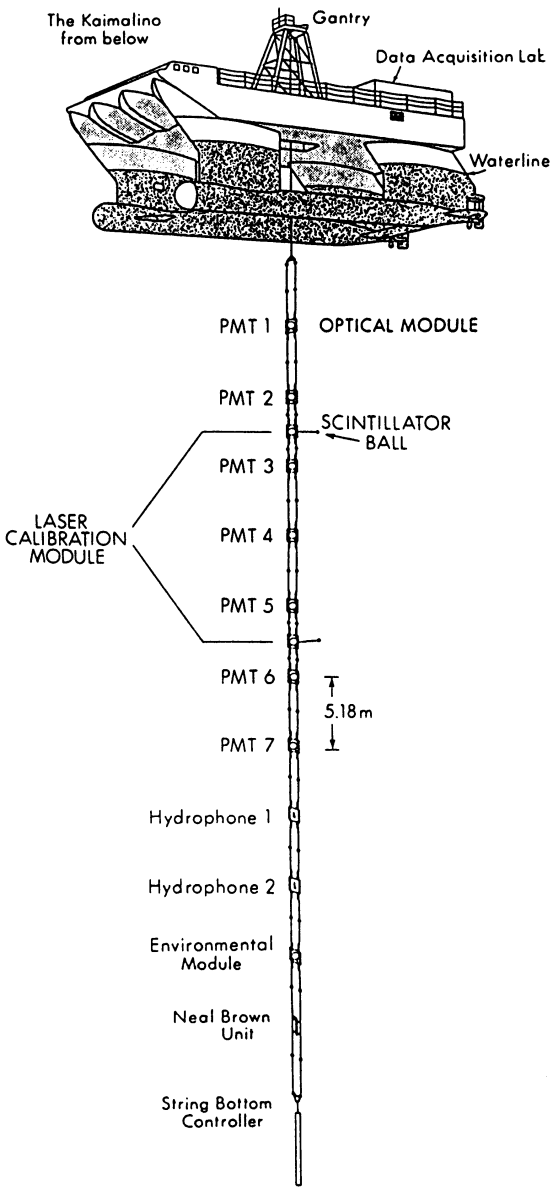

FIG. 1. Mechanical configuration of the short prototype string. Optical module spacing is 5.18 m.

(FWHM)] from the laser is optically coupled through a fiber bundle to a scintillation ball 2 m distant from the string axis. A photodiode in the calibration module monitors the laser output and has its signal injected into the data stream in exactly the same way as an optical module.

The arrival time and width of the optical module output pulse are digitized in the string bottom controller using 14 bits and 8 bits respectively, each with a least count of 5 ns. The digitized data of the optical-module pulses are combined with the module address bits, several flag bits, and a parity bit to form 32-bit data words.

Onboard ship, the serial data stream from the string bottom controller is converted to 32-bit parallel that forms a bus which is connected to CAMAC modules that monitor and process the data. One of these modules is a specially designed circuit called the trigger processor. The trigger processor continuously checks the incoming optical module data and generates a trigger pulse whenever a preprogrammed condition is satisfied. In the present experiment, the trigger condition required more than four or five optical modules to have a hit within a 160-ns time window. Concurrently, the data on the parallel data bus are stored in two 4000-word buffer memories. When the trigger processor generates a trigger pulse the data-taking system waits for 1 ms to ensure that any late hits associated with the event are loaded into the buffer memories; it then checks the contents of the buffer memories to find appropriate optical-module hits. Those optical-module hits, whose arrival times are within ± 250 ns of the hit that caused the trigger, are recorded to ensure that no optical-module data corresponding to the same muon are lost. The trigger rate was typically less than 10 Hz and the data-taking system had adequate time to process every trigger.

A steel armored cable of 7.9 mm diameter was used to suspend the string. Inside the armor, a polyethylene-insulated, 0.6-mm copper tube served as a 60-Hz ac power line for the instrument (0.7 kV A delivered) and also provided a 300-baud communication channel. The seawater-return technique was used for the ac power and communication signal ground. The cable was just over 4.0 km in length, limiting our maximum depth. The hollow central core of the copper conductor also served as a housing for a single-mode optical fiber. The fiber provided the 50-Mbaud optical data link from the string to the ship.

High-voltage (HV) ac power, delivered from the ship, is converted to 110 V ac at the string. Regulated dc power for the modules and string bottom controller electronics is derived from the 1000 V ac. The 300-baud communication signals are separated from the HV ac power, received at the string bottom controller, and then forwarded via a microprocessor in the string bottom controller to each module through two communication lines between the string bottom controller and the modules.

Each module on the string was monitored and controlled through the 300-baud communication channel with commands from the ship. Photomultiplier high-voltage and discriminator levels were set and monitored remotely from the surface. The counting rates, power supply voltages, temperature, anode current of the photomultiplier tubes, as well as various other instrumental data were monitored through the communication network. In the calibration modules both the intensity and repetition rate of the laser were controlled. At the two shallower depths, high voltage supplied to photomultiplier tubes was reduced from the standard value (nominal gain $=10^7$) in order to cope with higher background noise level due to bioluminescence. The differences in photomultiplier tube gain at these depths is taken into account in calculating the effective detection area.

III. THE EXPERIMENT

Previous studies on background light in the deep ocean[21-23] indicate that mechanical coupling of surface swell from the ship to the instrument through the tether cable results in an increase of more than one order of magnitude in background light levels due to stimulated bioluminescence, when compared with levels from an instrument anchored to the ocean floor. To minimize this effect, the string was deployed from a SWATH (small-water-area twin-hull) ship, the semisubmerged platform Kaimalino.[24] The measured vertical acceleration of the ship did not exceed $0.06g$ during the entire deployment. An hydraulic cable tension compensation system further reduced the motion of the modules. The accelerometer in the instrumentation module never recorded accelerations exceeding $0.03g$. Nevertheless, the instrument was in nearly continuous motion with a typical amplitude of 1 m and period of $\simeq 10$ s due to the ocean swell.

The experiment was conducted in the ocean $\simeq 30$ km off the west coast of the Island of Hawaii (156°27′ W, 19°42′ N) from 2 to 10 November 1987. The depth of the ocean floor at the site was measured to be 4.8 km. The string was lowered to each specified depth, and then left there while sufficient data were taken to reconstruct the muon intensity and angular distribution at that depth. The depths and observation times are listed in Table I. During the observation time of the short prototype string experiment, about 38 h total, 1.2×10^6 event triggers were recorded.

The depth of the instrument was determined using an acoustic transponder system. The ship-to-instrument round-trip travel time of a 12-kHz pulse was recorded. Travel time was corrected for effects due to salinity, temperature, and pressure, and the depth computed. The overall uncertainty in depth by this method is $\pm 1\%$.[25,26] As a check, the acoustical depths were compared to depths recorded using a mechanical cable meter. These methods agree to $\pm 2\%$. We assume an error of $\pm 2\%$ in all subsequent analysis.

IV. MUON RECONSTRUCTION

Each event recorded on the magnetic tape consisted of several to ten hits from optical modules, including false hits due to photomultiplier tube noise and background light from seawater radioactivity (^{40}K) and bioluminescence in the ocean. In off-line analysis, both time and intensity information from each hit were used to determine

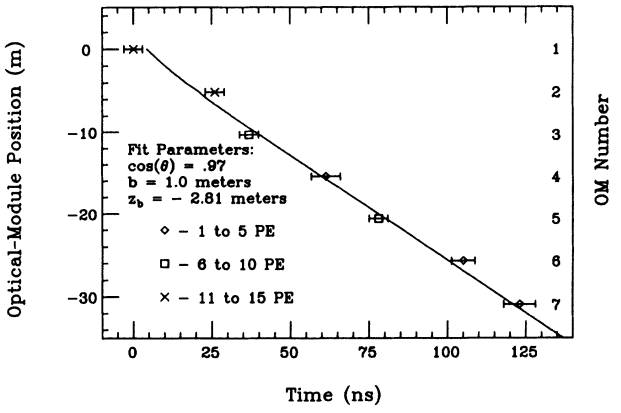

FIG. 2. Timing data and fit for typical muon event.

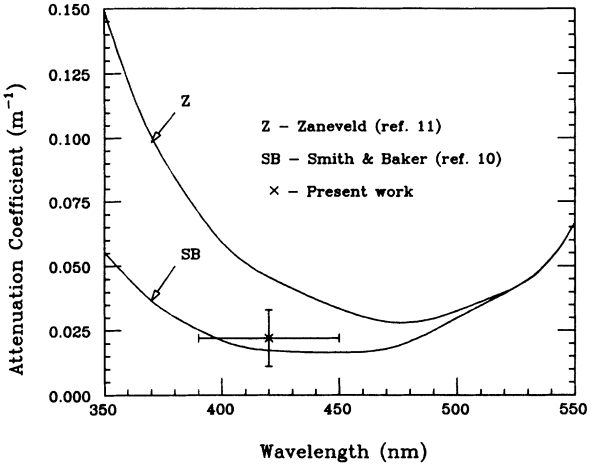

FIG. 3. Optical transparency of ocean water as determined by short prototype string calibrations compared with measurements of Smith and Baker (Ref. 11), and Zaneveld (Ref. 12).

the most probable muon trajectory. In order to reduce the background from false hits prior to muon reconstruction, hits with pulse widths shorter than the equivalent of 0.8 photoelectrons were rejected. Background was further reduced by selecting that group of hits having the maximum number within a 160-ns time window, the interval over which the hits can be causally related. A minimum-χ^2 fit was then performed to determine the best values of the parameters defining the muon trajectory: zenith angle θ, impact parameter b, and vertical coordinate of the point of closest approach z_b.

A typical muon event with time fit is shown in Fig. 2. The solid line shows the arrival-time pattern expected from the fit of the reconstructed muon. Because the conical wave front of the Cherenkov light from the muon, rather than a muon track itself, is detected, the arrival time pattern represents a hyperbolic segment.

The muon track fit is accepted for events in which at least five optical module hits give a fit with a χ^2 per degree of freedom ($N_{\rm DF}$) less than 3. In cases where $\chi^2/N_{\rm DF}$ exceeds 3, and there are more than five optical module hits, a second attempt is made to find a muon trajectory by removing the hit with the largest residual χ^2. Since the short prototype string has only a single string of detectors, the azimuthal angle is undetermined. From timing information alone, a twofold ambiguity exists in the zenith angle. However the light intensity information included in the χ^2 resolves this ambiguity in most cases.

The resulting numbers of reconstructed muon events and the measured muon event rates at each depth are shown in Table I.

TABLE I. Data summary.

Ocean depth (m)	Overburden (m.w.e)	Live time after cuts (sec)	Fivefold recon	Muon event rate (s^{-1})
2035	2090	179	13	$7.3\pm2.0\times10^{-2}$
2564	2633	7315	414	$5.6\pm0.34\times10^{-2}$
3077	3160	488	23	$4.7\pm0.97\times10^{-2}$
3610	3707	1704	99	$5.8\pm0.58\times10^{-2}$
4048	4157	5826	99	$1.7\pm0.18\times10^{-2}$

V. EFFECTIVE AREA AND ANGULAR SENSITIVITY

The effective detection area of the short prototype string was determined using a Monte Carlo calculation in which all known instrumental characteristics were simulated.[27] The optical modules were calibrated in the laboratory, so that their absolute sensitivity and angular response were known. The transparency of the water at the site was previously measured.[10,11] A spectral transmission function consistent with these observations (attenuation coefficient $=0.0286$ m^{-1} for $\lambda=450$ nm), was used for the simulations. Water transparency was also measured in this experiment, using the pulsed laser light (380–460 nm) from the calibration modules in the string. By analyzing the pulse-height response of the optical modules to laser light pulses, the attenuation coefficient of water was deduced to be 0.022 ± 0.011 m^{-1}. The result is shown in Fig. 3, along with results from previous measurements.

Monte Carlo event samples were generated both isotropically in zenith angle and with the angular distribution expected for cosmic rays at the given depth. For a given zenith angle θ, the events were generated uniformly in a cylinder with a large radius R, and axis oriented at that angle. The effective area for triggers was then calculated as $A_T(\theta)=f(\theta)\pi R^2$, where $f(\theta)$ is the fraction of simulated events which pass all the trigger criteria. Trigger conditions included a minimum fivefold coincidence at the 0.8-photoelectron level within a coincidence window of 160 ns. The result for $A_T(\theta)$ is shown in Fig. 4.

The fraction of these triggers which give a successful track reconstruction, defined as $\epsilon(\theta)$, is shown in Fig. 5. The effective area for fully reconstructed muons then is $A_F=\epsilon(\theta)A_T(\theta)$. For downward-going muons, $A_F(0)=420\pm87$ m^2 for fivefold coincidences where the error estimated mostly results from systematic uncertainty in the optical absolute sensitivity. The effective area averaged over the expected angular distribution of cosmic ray muons is $\langle A_F\rangle=322\pm67$ m^2. The loss of detec-

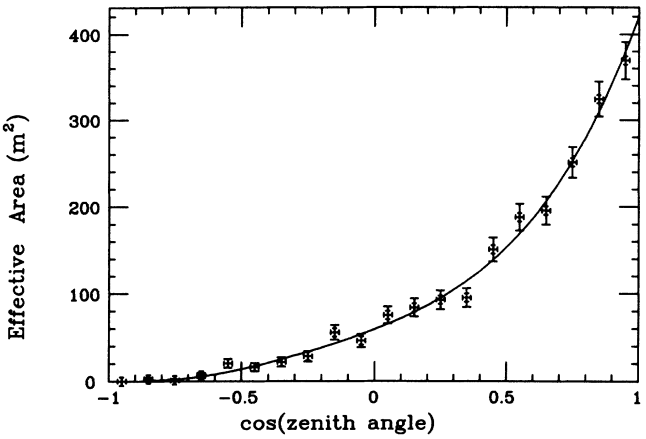

FIG. 4. Effective detection area for muons vs zenith angle.

tion efficiency with increasing zenith angle has two sources: (1) the angular response of the optical module falls off with polar angle ψ as $0.52+0.48\cos\psi$, so the detector is less sensitive to large zenith muons; (2) the timing of each module was adjusted in such a way that all modules generate a signal almost simultaneously for downward-going muons so, although a wide 160-ns time window is used, some upward muons would have been lost. This effect is included in the Monte Carlo simulation to calculate an expected muon angular distribution at a particular depth.

It should be noted that the determination of the effective detector area for the small single string of modules in this experiment is necessarily more uncertain than that for the large three-dimensional array of over 200 optical modules ultimately contemplated for DUMAND. In the latter case, the effective area will be close to the geometrical projected area, with the Monte Carlo simulation merely being asked to provide an estimate of the detection efficiency for through-going muons. Here we had the more difficult task of estimating the effective cross-sectional area of a column of water within which muons would successfully trigger and reconstruct in a linear array of only seven modules.

The Monte Carlo simulation was also used to estimate the angular resolution of the short prototype string detector by comparing the initial Monte Carlo parameters with the fit results. The distribution of the error in $\cos\theta$, where θ is the zenith angle, has a FWHM of 0.1 at $\cos\theta=1$, increasing to 0.3 at $\cos\theta=0$.

VI. DATA SELECTION AND LIVETIME

Even trigger rates and individual optical module counting rates were recorded each second on magnetic tape. The former was used to calculate the live time of the system by comparing it with the rate of analyzed muon data.

Off-line data selection was carried out in the following manner. First, the majority of runs in which a four-fold trigger was used were rejected due to a problem in synchronizing the second-by-second tube rates with the event trigger. This problem arose when the event trigger rate was too high and the data-acquistion system was not able to read individual tube rates every second. This was not a problem for the fivefold data since the event trigger rate was much lower. Portions of runs which contained a calibration sequence were eliminated. The combination of these two cuts eliminated a large fraction of the raw data.

The data link between the string bottom controller and the ship had a capacity of 50 Mbaud. The data transfer rate was limited to about 1.4×10^6 data words per second since each optical-module pulse was converted to a 29-bit word and 80 ns was needed between data words to ensure that there was no overlap. If the total optical module rate exceeded this value for some time, the string-bottom-controller data stack (16 words deep) overflowed resulting in the loss of data. Data from the magnetic tape were analyzed only when the total noise rate of all optical modules was less than 1 MHz, to eliminate incomplete events. This cut eliminated about 30% of the remaining fivefold data at 4000 m.

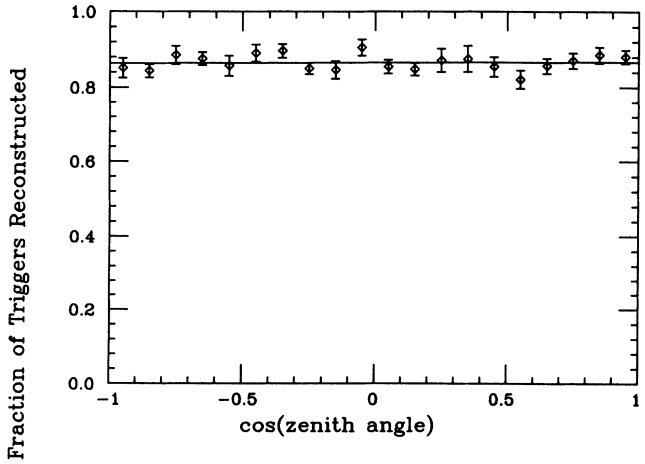

FIG. 5. Muon track fitting efficiency vs zenith angle.

VII. RESULTS

A. Depth-intensity relation

Using the effective detection area determined by the Monte Carlo simulation shown in Fig. 4, the events rates in Table I can be converted into a total muon intensity as a function of depth. In order to compare with other measurements, we have constructed these to vertical intensities using a correction factor supplied by Kobayakawa.[28] This comparison is given in Table II and is illustrated in Fig. 6. The figure also shows a comparison with an empirical formula of Miyake derived from the results of underground measurements,[29] converted to seawater to account for the differences in energy loss between sea water and rock.[30–32] A more accurate calculation for seawater by Inazawa and Kobayakawa[33] is also shown in this figure. The data points plotted are limited to depths greater than 1000 m.

TABLE II. World undersea muon data at depths greater than 500 m. NA denotes "not available."

Group	Location	$\langle\rho\rangle$	$\langle Z\rangle$	$\langle A\rangle$	$\langle Z/A\rangle$	$\langle Z^2/A\rangle$	Depth (mwe)	Depth error (%)	Time (sec)	N events	$\frac{\sqrt{N}}{N}\times 100$	$\langle\text{Area}\rangle_\theta$ (m^2)	Vert. intensity ($cm^{-2}s^{-1}sr^{-1}$)
Higashi 66	W. Pac.	1.027	7.433	14.787	0.553	3.76	715	±2	NA	NA	NA	6	$2.30\pm0.20\times10^{-6}$
(Ref. 12)	Suruga Bay						960	±2	NA	NA	NA	6	$7.50\pm0.66\times10^{-2}$
	34.5° N, 138.5° E						1380	±2	NA	NA	NA	6	$3.50\pm1.40\times10^{-7}$
Vavilov 70	Black sea	NA	7.43	14.78	0.553	3.76	1090	1–3	34 200	375	5.2	1.2	$6.0\times0.31\times10^{-7}$
(Ref. 15)	NA° N, NA° W												
	Mediter.						1970	1–3	56 700	126	8.9	1.2	$1.45\pm0.13\times10^{-7}$
	37.9° N, 18.9° E												
	Atlantic						3190	1–3	332 100	114	9.4	1.2	$2.55\pm0.23\times10^{-7}$
	37.3° N, 10° W												
Fyodorov 85	Carib.	NA	NA	NA	NA	NA	2925	1–3	19 800	1304	2.8	50	$3.1\pm0.5\times10^{-8}$
(Ref. 13)	19° N, 76° W												
	Atlantic						4025	1–3	28 800	417	4.9	50	$5.9^{+2.0}_{-2.5}\times10^{-9}$
	22° N, 37° W												
							5020	1–3	115 200	168	7.7	50	$4.1^{+1.6}_{-2.0}\times10^{-9}$
DUMAND													
88	C.Pac.	1.027	7.468	14.869	0.5525	3.77	2090	1	179	13	27.7	121	$9.84\pm6.5\times10^{-8}$
	Kona						2633	1.1	7315	414	4.9	121	$8.04\pm3.3\times10^{-8}$
	19.7° N, 156.5° W						3160	1.4	488	23	20.8	210	$2.04\pm0.83\times10^{-8}$
							3707	2.1	1704	99	10.0	316	$1.31\pm0.40\times10^{-8}$
							4157	0.3	5826	99	10.0	322	$4.57\pm1.32\times10^{-9}$

B. Muon angular distribution

Our measured muon angular distribution at 4157 meters of water equivalent (mwe) is shown in Fig. 7. The solid line shows the expected angular distribution, obtained from running Monte Carlo simulated events through the same software used to analyze the real data, so that the nonisotropic effective area and fitting efficiencies shown in Figs. 3 and 4 are taken into account. Events beyond zenith angle of 90° arise due to misfit muons in the reconstruction program (caused by fluctuations in muon energy loss and in detection response).

Muon intensity as a function of zenith angle, and at a fixed depth can be modeled by $I(\theta)=I_0\cos^n(\theta)$, where n is an index. A maximum-likelihood fit, using Poisson probabilities, to the angular distribution data at 4157 mwe has been done to determine the best value of n. A Monte Carlo sample of muons, generated with a fixed n, is processed through the muon fitter to produce a distribution that can be compared to the short prototype string measurements. The resulting distribution is smoothed

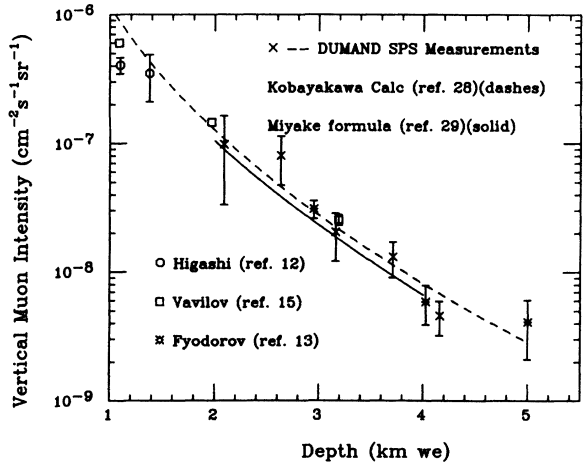

FIG. 6. Measured muon vertical intensity vs depth compared with other underwater experiments below 1000 m depth. The errors indicated are both systematic and statistical.

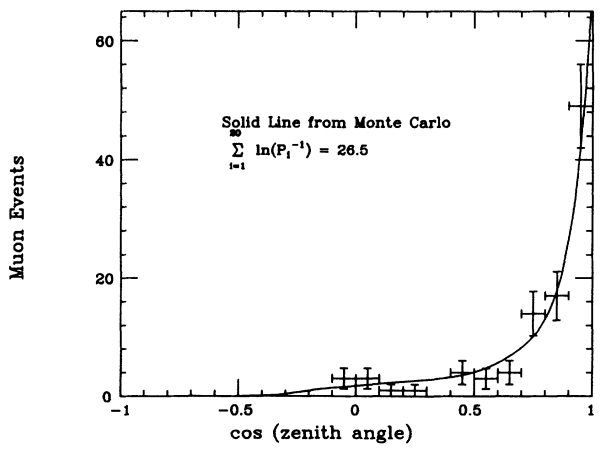

FIG. 7. Measured muon angular distribution at 4 km. The vertical error bars are just statistical.

and scaled to the short prototype string measurement. The scaling is determined by a maximum-likelihood fit of the Poisson probability of obtaining the observed number of events in each bin, where the expected number in each bin is the scaled value of the generated number. The confidence level of the best fit was determined by calculating the likelihood for each of a set of Poisson fluctuations from the best fit angular distribution. We determine a value for $n=6^{+7}_{-1}$, consistent with a previous measurement by Achar *et al.*[34,35] at 4100 m of 5.12 ± 0.82.

C. Fit to energy-loss parameter b

The mean muon energy loss in a medium can be parametrized by $-dE/dx=a_{\rm ion}(E)+b(E)E$, where E (TeV) is the muon energy, and x is the distance traveled in the medium (g cm^{-2}). Continuous energy losses due to ionization and atomic excitation are given by $a_{\rm ion}$.[36] Losses due to pair production, bremsstrahlung, and nuclear interactions are contained in $b(\text{km}^{-1})=b_{\rm pair}+b_{\rm brem}+b_{\rm nuclear}$. Using the approximation that both $a_{\rm ion}$ and b are independent of energy we integrate the loss equation and solve for range vs energy. Inversion yields $E=a/b\,[\exp(bx)-1]$. We now parametrize the integral vertical muon flux as $\Phi=\Phi_0(E/E_0)^{-\beta}$, where β is the integral muon spectral index, and E_0 is the normalization energy. Combining the $E=E(x)$ equation with the integral flux equation allows us to fit our data for $b_{\rm eff}$, the effective catastrophic energy loss term. We employ a χ^2-minimization process to determine values of $b_{\rm eff}$ for a range of indices, $2.58\le\beta\le2.67$. The resulting fit for a central value $\beta=2.625$ gives $b_{\rm eff}=0.440\pm0.028$ and is shown in Fig. 8. This result is consistent with a fit to the theoretical calculation of Kobayakawa, if we assign them the same errors as our own experimental data [$b_{\rm eff}$(KK)$=0.300\pm0.137$].

In Fig. 9 (see also Table II) we fit a compilation of the world undersea muon data at depths greater than 1000 m. A robust fit (reject data with $\chi^2>10$) for the world data gives $b_{\rm eff}(\beta=2.625)=0.361\pm0.046$.

VII. COMPARISONS AND DISCUSSION

As shown in Fig. 6 our result on the muon depth-intensity relation is consistent with Miyake's empirical formula converted to equivalent range for seawater.[37] This formula was determined by fitting the data from underground experiments and well represents these data down to 7000 hg/cm^2. A recent compilation of muon depth intensity data underground[38] gives results indistinguishable from Miayke's formula ($\pm3\%$) for depths between 1 and 5 km. Thus our results are consistent with underground results.

The angular distribution of muons at 4000 m depth is also consistent with the expected distribution derived from the Miyake formula. At larger zenith angles, this corresponds to slant depths greater than 4 km corresponding to muon energies at sea level greater than 2 TeV.

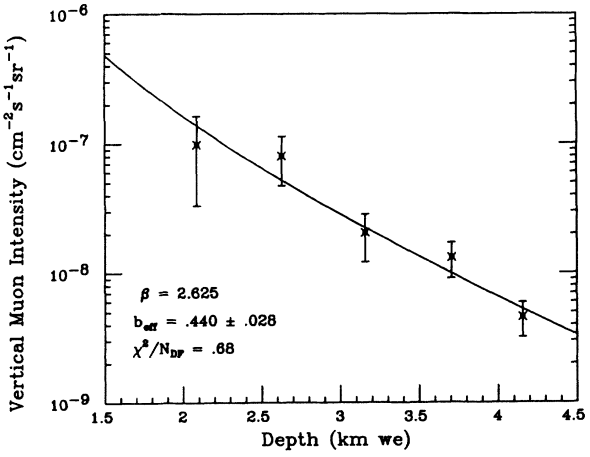

FIG. 8. Fit to short prototype string vertical muon intensity data for $b_{\rm eff}$.

IX. CONCLUSION

Cosmic-ray muons in the deep ocean have been detected and their trajectories have been reconstructed using a ship-deployed water Cherenkov muon telescope. The telescope consists of a string of seven photomultiplier tubes spaced 5.18 m apart. The basic detection technique proposed for the DUMAND project has been verified in one of the most technically sophisticated experiments ever performed in the deep ocean. The effective detection area of the short prototype string for downward-going muons, was 420 m^2—larger than any previous experiment underwater or underground, except for the Irvine-Michigan-Brookhaven proton-decay detector.[39,40] Muon fluxes were determined at 500 m incremental depths ranging from 2000 to 4000 m and the angular distribution was measured (for the first time ever) at a great depth in the ocean.

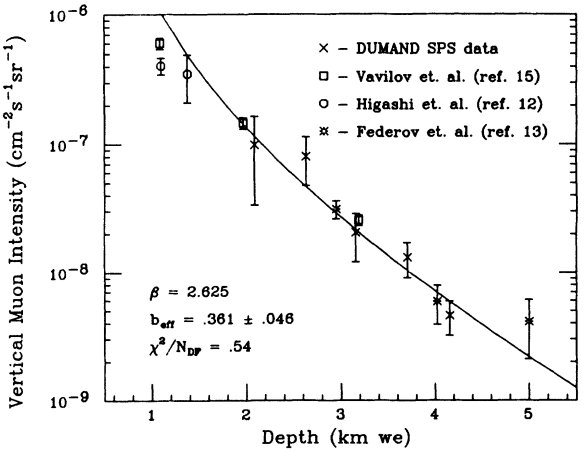

FIG. 9. Fit to compilation of world undersea vertical muon intensity data $b_{\rm eff}$.

The reported results are consistent with underground measurements and theoretical calculations for the absolute muon fluxes and angular distributions at each depth. The flux at a depth of 4157 mwe is measured to be $[4.57\pm0.46(\text{stat})\pm0.91(\text{sys})]\times10^{-9}\ \text{cm}^{-2}\,\text{s}^{-1}\,\text{sr}^{-1}$.

ACKNOWLEDGMENTS

We are deeply indebted to Captain C. Gudzeit, H. Chalmers, and the able crew of the Kaimalino. We are especially indebted to J. Elliott, D. Harris, R. Mitiguy, M. Rosen, G. Wilkins, and P. Yuen for their invaluable contributions to this experiment. We would like to express our thanks to G. Blackinton, Y. Miyakoshi, L. Kelly, T. Aoki, C. Helsley, J. Hudson, N. Kamikawa, M. Lapolla, M. Matsunaga, M. McMurdo, A. Nakagawa, G. H. Sembrowski, G. Shetler, H. Talkington, and R. Tom, for their assistance at various stages of the project. We thank K. Kobayakawa for valuable discussions and calculations in support of this analysis. We are also grateful for the support and encouragement obtained from the Hawaii Institute of Geophysics and the Naval Ocean Systems Center at Kaneohe. We thank the Irvine-Michigan-Brookhaven Collaboration for use of their detector in doing a tagged-muon, absolute sensitivity calibration of the optical modules. This research was supported by the particle-physics divisions of the U.S. Department of Energy, the U.S. National Science Foundation, the Swiss National Science Foundation, and by a Grant in Aid for Scientific Research from the Japanese Ministry of Education, Science, and Culture.

---

*Present address: Los Alamos Scientific Laboratory, Los Alamos, NM 87545.

†Present address: Boston University, Boston, MA 00215.

‡Present address: California Institute of Technology, Pasadena, CA 91125.

§Present address: Research Institute for Science and Technology, Kinki University, Higashi-Osaka, Japan.

[1]S. Matsuno *et al.*, Phys. Rev. D **29**, 1 (1984).

[2]O. C. Allkofer *et al.*, in *Proceedings of the 17th International Cosmic Ray Conference*, Paris, France, 1981 (CEN, Sarclay, 1981), Vol. 10, p. 321.

[3]O. C. Allkofer *et al.*, Phys. Rev. Lett. **36B**, 425 (1971).

[4]C. A. Ayre *et al.*, J. Phys. G **1**, 584 (1975).

[5]For a compilation of data, see O. C. Allkofer and P. K. F. Grieder, *Cosmic Rays on Earth* (Fachsinformationszentrum, Karlsruhe, 1984).

[6]M. R. Krishanswamy *et al.*, in *Proceedings of the 15th International Conference on Cosmic Rays*, Plovdiv, Bulgaria, 1977, edited by B. Beter (Bulgarian Academy of Science, Plovdiv, Sofia, 1977), Vol. 7, p. 85.

[7]M. F. Crouch *et al.*, Phys. Rev. D **18**, 2239 (1978).

[8]W. R. Shelden *et al.*, Phys. Rev. D **17**, 114 (1978).

[9]V. M. Goldschmidt, *Geochemistry* (Clarendon, Oxford, 1954), p. 49.

[10]R. S. Smith and K. S. Baker, Appl. Opt. **20**(2), 177 (1981).

[11]J. R. Zaneveld, in *DUMAND 80*, proceedings of the Symposium, Honolulu, Hawaii, 1980, edited by V. J. Stenger (Hawaii DUMAND Center, Hawaii, 1980), Vol. 1, p. 1.

[12]S. Higashi *et al.*, Nuovo Cimento **43A**, 334 (1966).

[13]V. M. Fyodorov *et al.*, in *Proceedings of the 19th International Cosmic Ray Conference*, La Jolla, California, 1985, edited by F. C. Jones, J. Adams, and G. M. Mason (NASA Conf. Publ. 2376) (Goddard Space Flight Center, Greenbelt, MD, 1985), Vol. 8, p. 39.

[14]H. F. Davis and J. G. Learned, Phys. Rev. D **8**, 8 (1973).

[15]Yu. N. Vavilov *et al.*, Bull Acad. Sci. USSR **34**, 1759 (1970).

[16]DUMAND proposal, Report No. HDC-3-88, 1988 (unpublished), available from Hawaii DUMAND Center.

[17]R. Becker-Szendy, DUMAND Report No. DIR-5-87, 1987 (unpublished), available from Hawaii DUMAND Center.

[18]S. Matsuno *et al.*, Nucl. Instrum. Methods A **276**, 359 (1989).

[19]Doctoral dissertations of D. O'Connor and J. F. Babson, University of Hawaii, and J. Clem, Vanderbilt University (in preparation).

[20]Photomultiplier tube type R-2018, Hamamatsu Photonics, Hamamatsu, Japan.

[21]T. Aoki *et al.*, Nuovo Cimento **9C**, 624 (1986).

[22]H. Bradner *et al.*, Deep-Sea Res. **34**, 1831 (1987).

[23]A. V. Abin *et al.*, in *Proceedings of the 20th International Cosmic Ray Conference*, Moscow, USSR, 1987, edited by V. A. Kozyarivsky *et al.* (Nauka, Moscow, 1987), Vol. 6, p. 237.

[24]J. D. Hightower and R. L. Seiple, Report No. 78-741 at American Institute of Aeronautics and Astronautics–Society of Naval Architects and Marine Engineers, Advanced Marine Vehicles Conference, San Diego, 1978 (unpublished).

[25]A. Lewitus, DUMAND Report No. DIR-14-83 (unpublished), available from Hawaii DUMAND Center.

[26]W. Wilson, J. Acoust. Soc. Am. **32**, 641 (1960).

[27]V. J. Stenger, DUMAND Report No. DIR-2-86 (unpublished), available from Hawaii DUMAND Center.

[28]K. Kobayakawa (private communication).

[29]S. Miyake, J. Phys. Soc. Jpn. **18**, 1093 (1963).

[30]A. G. Wright, in *Proceedings of the 13th International Conference on Cosmic Rays*, Denver, Colorado, 1973 (Colorado Associated Univ. Press, Boulder, 1973), Vol. 3, p. 1709.

[31]M. G. K. Menon and P. V. Ramana Murthy, Prog. Elem. Part. Phys. **9**, 163 (1967).

[32]K. Kobayakawa, Can. J. Phys. **45**, S395 (1968).

[33]H. Inazawa and K. Kobayakawa, in *Proceedings of the 19th International Cosmic Ray Conference* (Ref. 12), p. 83.

[34]C. V. Achar *et al.*, Proc. Phys. Soc. **86**, 1305 (1965).

[35]J. N. Crookes and B. C. Rastin, Nucl. Phys. **B58**, 93 (1973).

[36]K. Kobayakawa, Nuovo Cimento **47**, 840 (1967).

[37]M. G. Thompson and M. R. Whalley, J. Phys. G **1**, L1 (1975).

[38]M. Crouch, in *Proceedings of the 20th International Cosmic Ray, Conference* (Ref. 23), p. 165.

[39]R. M. Bionta *et al.*, Phys. Rev. Lett. **51**, 27 (1983).

[40]R. C. Svoboda, Ph.D. thesis, University of Hawaii, 1985.

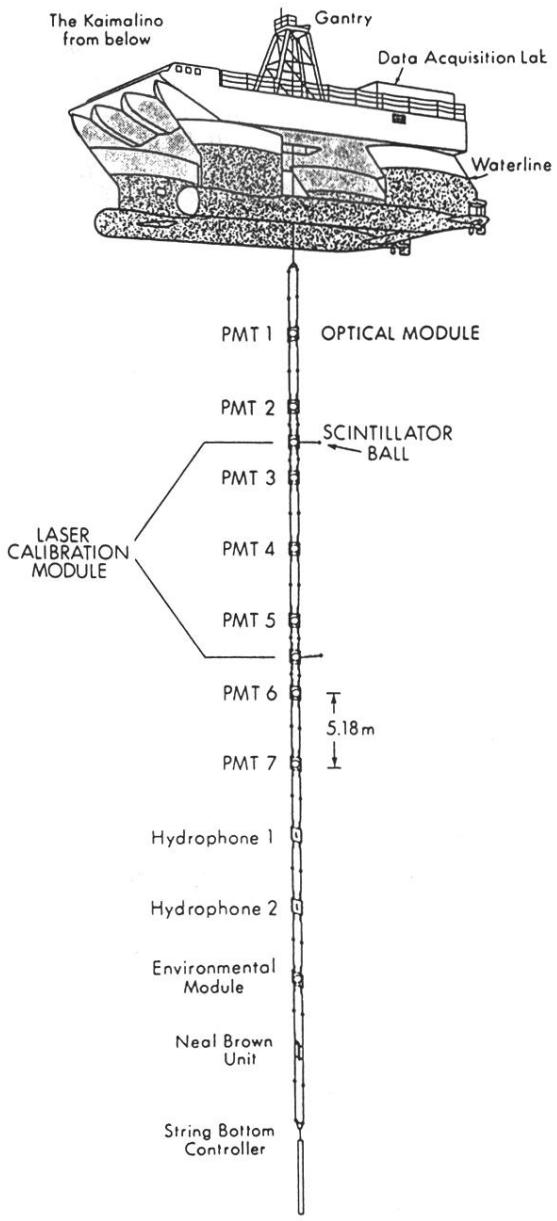

FIG. 1. Mechanical configuration of the short prototype string. Optical module spacing is 5.18 m.